

Research Article

Investigate the Effect of Coating Concentration and Coating Thickness on the Anti-microbial Properties of Polycarbonate Sheet

Saleh Alkarri*

School of Packaging, Michigan State University, 448 Wilson Road, East Lansing, MI 48824-1223, USA

Abstract

This paper investigates the effect of coating concentration (ppm), and coating thickness (μm) on the anti-microbial properties of polycarbonate sheets using a variety of anti-microbial agents (Cu-infused $\text{Mg}(\text{OH})_2$, $\text{Mg}(\text{OH})_2$, $\text{Cu}(\text{OH})_2$, MgO , $\text{CuCl}_2 \cdot 2\text{H}_2\text{O}$, and ZnO). In addition, a complete analysis was performed for all agents to rank the best agent in terms of the highest anti-microbial performance against *E. coli* K-12 MG1655 in two time intervals (4 and 24 hours). The coating concentration (ppm) was found to be a significant factor in the anti-microbial characteristics for Cu-infused $\text{Mg}(\text{OH})_2$, $\text{Mg}(\text{OH})_2$, $\text{Cu}(\text{OH})_2$, MgO , $\text{CuCl}_2 \cdot 2\text{H}_2\text{O}$, and ZnO ($p = 0.004$, $p < 0.0001$, $p < 0.0001$, $p = 0.0297$, $p = 0.0011$, and $p = 0.0130$ respectively). The coating thickness (μm), on the other hand, was found to be a major contributor to the anti-microbial properties of Cu-infused $\text{Mg}(\text{OH})_2$, $\text{Mg}(\text{OH})_2$, $\text{Cu}(\text{OH})_2$, MgO , and $\text{CuCl}_2 \cdot 2\text{H}_2\text{O}$ ($p < 0.0001$, $p = 0.0004$, $p = 0.0011$, $p = 0.0310$, and $p < 0.0001$ respectively). The analysis determined that the coating did not influence the anti-microbial properties of ZnO . The interaction between the coating concentration (ppm), and the coating thickness (μm) was found to be a significant factor for Cu-infused $\text{Mg}(\text{OH})_2$, $\text{Cu}(\text{OH})_2$, MgO , $\text{CuCl}_2 \cdot 2\text{H}_2\text{O}$, and ZnO ($p < 0.0001$, $p = 0.0001$, $p = 0.0004$, $p < 0.0001$, and $p < 0.0001$ respectively), however, this was not a significant factor for $\text{Mg}(\text{OH})_2$.

Highlights

- The anti-microbial activity of the inorganic material is dependent on the particle shape and size.
- Particles with sharp edges will provide additional physical injuries to the microorganisms.
- Smaller particle size will provide higher surface area therefore better interaction with microorganisms.
- The coating concentration and coating thickness will be crucial to the anti-microbial activity.
- The thermal embossing techniques demonstrate good adhesion to the surface.

Introduction


Surface touch and air movement can transfer microorganisms, contributing to the spread of infectious diseases. When people come into contact with contaminated surfaces, bacteria can adhere to their hands, allowing them to spread to other surfaces or enter the body [1]. Coughing into one's hand and touching a doorknob, for example, can spread respiratory germs [2]. Another person who touches the same doorknob and then touches their face can transmit bacteria into their respiratory system [3]. Furthermore, air movement, particularly aerosols, enables microbes to fly through the air and potentially reach distant areas [4]. Hand hygiene

and surface disinfection are critical in reducing microbial transmission.

Bacterial growth on surfaces is an issue, given the ease of microbial transfer. Bacterial growth on surfaces, in essence, constitutes a serious severe concern, leading to the formation of biofilms and possible diseases [5]. Anti-microbial surfaces are critical for minimizing the risk of infection transmission and inhibiting bacterial colonization [6]. These surfaces are used in medical settings, food processing areas, and high-touch surfaces. Surface anti-microbial coatings or compounds can effectively suppress bacterial growth and survival, reducing the risk of infection [7-9]. They provide benefits

More Information

*Address for correspondence: Saleh Alkarri, School of Packaging, Michigan State University, 448 Wilson Road, East Lansing, MI 48824-1223, USA, Email: alkarri@msu.edu

 <https://orcid.org/0009-0003-3549-9585>

Submitted: May 22, 2024

Approved: May 28, 2024

Published: May 29, 2024

How to cite this article: Alkarri S. Investigate the Effect of Coating Concentration and Coating Thickness on the Anti-microbial Properties of Polycarbonate Sheet. *Ann Biomed Sci Eng.* 2024; 8: 011-020.

DOI: 10.29328/journal.abse.1001029

Copyright license: © 2024 Alkarri S. This is an open access article distributed under the Creative Commons Attribution License, which permits unrestricted use, distribution, and reproduction in any medium, provided the original work is properly cited.

Keywords: Anti-microbial activity; *E. coli* K-12 MG1655; Thermal embossing; Coating concentration; Coating thickness



such as decreasing microbial contamination, avoiding biofilm formation, and improving surface hygiene. Developing anti-microbial surfaces is crucial for ensuring safe environments, especially in healthcare settings where infection control is paramount [7].

Organic anti-microbial agents are anti-bacterial compounds derived from natural or synthetic sources. Thymol ($C_{10}H_{14}O$) is an organic anti-bacterial agent derived from thyme oil [10]. Organic chemicals have numerous advantages, including biodegradability, low toxicity, and compatibility with a wide range of polymer matrices [11]. They are easily incorporated into polymers using melt-compounding or coating methods. On the other hand, organic anti-microbial chemicals may be less durable, less effective against specific microorganisms, and have odor issues [9].

In contrast, non-carbon-based compounds make up inorganic anti-bacterial agents. A common inorganic anti-bacterial agent is silver nanoparticles (Ag NPs; symbol: Ag) [12]. Their advantages include strong potency against a range of pathogens, long-term stability, and broad-spectrum anti-bacterial activity. Since inorganic agents are compatible with melt-compounding and coating techniques, they can be included in polymers. However, they can raise environmental issues due to their possible toxicity and accumulation in the ecosystem [13].

Leachable anti-microbial agents are chemicals capable of being discharged or migrating from a material, such as plastics, into the surrounding environment or the target application. Silver ions (Ag^+) emitted from silver nanoparticles (Ag NPs), for example, are leachable anti-bacterial agents [14]. The benefit of leachable compounds is that they continuously release anti-bacterial activity, resulting in long-lasting efficacy. Their downside is that the active agent may be depleted with time, necessitating replenishment. Recent studies have concentrated on optimizing the controlled release of leachable anti-microbial compounds from polymers to assure long-term efficacy while limiting environmental impact [15]. Non-leachable anti-microbial agents, on the other hand, are immobilized or bonded to the material surface and do not release active agents into the environment. One example is the integration of magnesium hydroxide ($Mg(OH)_2$) nanoparticles into plastic surfaces [16]. Non-leachable compounds have the advantage of providing long-term anti-microbial protection without replenishment [7]. Their drawback, however, is that they may lose potency over time due to surface degradation or depletion of active sites [17]. To preserve anti-microbial efficacy, researchers are improving the adherence and longevity of non-leachable anti-microbial coatings on plastic surfaces [18].

Soluble anti-microbial agents can easily dissolve or disperse in a liquid medium. Triclosan ($C_{12}H_7Cl_3O_2$) is one such organic molecule [19]. Soluble compounds can rapidly and effectively

release anti-bacterial properties upon dissolution, resulting in immediate action against germs [20]. Their drawback is that they may leach out of the plastic matrix over time, resulting in decreased efficacy and environmental problems. On the other hand, non-soluble anti-microbial compounds stay intact or insoluble in a liquid medium while still demonstrating anti-bacterial characteristics. Ag NPs are one example [12]. Non-soluble compounds have the benefit of having long-lasting anti-bacterial activity since they are incorporated or coated into the plastic surface. This gives long-term resistance to microbial invasion. However, unlike soluble agents, the release of anti-microbial agents from the plastic matrix may be delayed and less efficient [21].

Recent research on anti-microbial agents for plastic applications has concentrated on optimizing their performance by striking a balance between solubility and stability. Studies on controlled release mechanisms and incorporation approaches for soluble compounds have been conducted to improve their lifespan and prevent leaching [7]. Mokabber, et al. studied non-soluble chemicals for surface modification strategies to improve adhesion and durability on plastic substrates [22]. These developments attempt to improve anti-bacterial efficacy while reducing potential downsides in plastic applications.

Although a variety of anti-microbial particles have been used in melt-compounding and coating technologies, the specific concentrations, thicknesses, and outcomes vary depending on the inquiry. For instance, $Mg(OH)_2$ nanoparticles functionalized with rosehip extract were employed by Alves, et al. showing an improved anti-bacterial activity against *Escherichia coli* (*E. coli*) [10]. In polyethylene films with embedded ZnO nanoparticles at 1% and 3% concentrations, Darvish and Ajji observed an inhibitory impact on *Staphylococcus aureus* (*S. Aureus*) and (*E.coli*) [23]. Plastic leachable and their analytical methods were studied by Cuadros-Rodriguez, et al. [19].

Anti-microbial coating concentration and thickness have a substantial impact on their effectiveness. Recent research has established this link. For example, Kania and Sipa studied the corrosion resistance of zinc coatings generated using a thermal diffusion technique, discovering that coating concentration affects anti-microbial characteristics [24]. Lin, et al. investigated the anti-bacterial capabilities of MgO nanostructures on magnesium substrates and discovered that coating thickness influenced bacterial growth suppression [25]. Mokabber, et al. investigated the anti-bacterial properties of silver-containing calcium phosphate coatings and discovered that the thickness of the coating influenced the level of bacterial inhibition [22].

The market size for anti-microbial agents in plastic applications is large and shows significant growth. For example, Mahanta, et al. emphasize the increased interest in

synthetic techniques for anti-microbial surfaces [7]. Birkett, et al. present improved anti-microbial metal-based coatings for high-touch surfaces [13]. Pinho, et al. present an overview of polymeric coatings with anti-bacterial action, highlighting the growing interest in this field [8].

Numerous studies have shown that $Mg(OH)_2$, $Cu(OH)_2$ and ZnO with Cu infusions showed higher anti-bacterial action against Gram-positive and Gram-negative pathogens. The anti-bacterial effectiveness of Cu-infused $Mg(OH)_2$ is increased because of the synergistic interaction of copper and magnesium ions, which disrupt bacterial membranes and obstruct biological activity [26]. Copper ions, produced by $Cu(OH)_2$, have anti-microbial properties. ZnO nanoparticles lead to oxidative stress and the death of bacterial cells. These findings, which show anti-bacterial efficiency against various bacterial species, were published by Alves, et al. Lin, et al. and Nakamura, et al. [10,25,27].

The anti-microbial particles have the following killing mechanisms: Mullen, et al. found that Cu-infused $Mg(OH)_2$ causes membrane rupture, intracellular ROS production, and magnesium ion interference [18]. Okamoto, et al. state that ZnO nanoparticles cause oxidative stress, DNA damage, and membrane disruption [28]. Tuson, et al. discovered that $Cu(OH)_2$ disrupts bacterial membranes and interferes with biological functions [1]. $Mg(OH)_2$ possesses anti-bacterial properties due to pH changes and the production of hydroxyl ions [29]. $CuCl_2 \cdot 2H_2O$ has been shown to denature proteins and damage cell membranes [13]. MgO nanoparticles display anti-bacterial capabilities via Reactive Oxygen Species (ROS) production and cell membrane breakdown [25].

Cu-infused $Mg(OH)_2$, $Cu(OH)_2$, MgO, $CuCl_2 \cdot 2H_2O$, and ZnO have varied FDA approval statuses. The FDA has not listed Cu-infused $Mg(OH)_2$, $Cu(OH)_2$, $CuCl_2 \cdot 2H_2O$, as approved [13]. The FDA has determined that $Mg(OH)_2$ is generally recognized as safe (GRAS) [30]. MgO nanoparticles have demonstrated low cytotoxicity and the potential for FDA approval [31]. Due to safety concerns, ZnO nanoparticles have yet to be approved by the FDA [29]. More research is required for a definitive FDA clearance status.

Experimental

Materials

Polycarbonate homopolymer (PC 0703R grade) pellets were gifted from SABIC (Riyadh, Saudi Arabia) as pellets having the following characteristics: melting point = 280 °C, density = 1.2 g/cm³, and melt flow index (MFI) = 7 g/10 min (300 °C/1.2 Kg). Isopropyl alcohol was obtained from Macron Fine Chemicals (purity: 99.99 %). Suppliers of all anti-microbial agents are listed in Table 1.

Preparation of all suspensions for coating

The preparation of all anti-microbial suspensions that were

used for thermal embossing is listed in (Table 1). After dilution and mixing, the suspension was vortexed at a maximum speed for 30 seconds, and subsequently sonicated in an ultrasonic bath (Branson 2510 Ultrasonic Sonicator, Commack, NY, USA) at 23 °C for 10 min to ensure that the NPs suspension was uniformly dispersed. After sonication, the suspension was vortexed once more at the maximum speed for 30 seconds.

Cast film extrusion

The PC pellets were used to make the flat PC sheet (Figure 1) using Randcastle extruders model RCP-0625 (5/8 inch 24:1 L/D), and 8-inch flex lip die. The barrel zone temperature was 280 °C, and the hopper temperature was 55 °C. The adapter temperature was 270 °C, and the die temperature was 280 °C. The extruded PC sheet was cut into a rectangular shape (dimensions: 20x30x0.03 cm) using Esko Kongsberg X-24 digital cutting table.

Metallic rod applicator for coating

A metallic rod applicator technique (K303, RK Print Coat Instruments Ltd., UK) was used to deposit the anti-microbial biocidal suspension over the extruded PC sheet (dimensions: 20x30x0.03 cm). The thickness of the wet deposited coating varied between 4-120 micrometers depending on the diameter of the wire (Table 2 and Figure 2). The anti-microbial suspension was spread as a wet film deposition over the extruded PC sheet (via 5 mL syringe) using the metallic rod applicator number (MRA No. 3 and 5), corresponding to a thickness of 24 and 50 microns (µm), respectively, and left to dry at 23 °C for 10 min.

Thermal embossing

The PC sheet which was temporarily coated with anti-microbial particles was sandwiched into an aluminum foil (All-Foils, Inc. OH, USA, Dimensions: 0.00762x30.48x30.48 cm) before the thermal embossing (Figure 3).

The thermal embossing technique for the temporarily deposited anti-microbial particles over the PC sheet was conducted using a compression molding (Figure 4) press (PHI QL438-C, City of Industry, CA, USA). A temperature of 205 °C and 2 bar of pressure for 10 s were used for the PC sheet. Disks were cut (dimensions: 20 mm in diameter, 0.05 mm in thickness) from PC sheets of thermally embossed particles, neat PC (without biocides) using a Kongsberg X24 Edge Cutting Table.

Anti-microbial testing methods

The anti-microbial properties of different PC films were tested according to the methods described in Alkarri, et al. [32] The *E. coli* K-12 MG1655 (American Type Culture Collection, Manassas, VA) was used for all experiments to evaluate the anti-microbial activities of the disks at 0, 4, and 24 hr intervals.

Table 1: The preparation of anti-microbial coating suspensions.

Compound Name	Purity (%)	Form of Compounds	Dilution	Final Concentration	Supplier
Cu-infused Mg(OH) ₂	99.99	Slurry dispersed in water: 7.47 wt.% Cu-infused Mg(OH) ₂ and 92.53 wt.% water	1.34 mL of Cu-infused Mg(OH) ₂ was diluted with 8.66 mL isopropyl alcohol	10 mg/mL	Aqua Resources Corp
Mg(OH) ₂	99.99	Slurry dispersed in water: 7 wt.% Mg(OH) ₂ and 93 wt.% water	14.3 mL of Mg(OH) ₂ was diluted with 85.7 mL isopropyl alcohol	10 mg/mL	Aqua Resources Corp
CuCl ₂ ·2H ₂ O	99.99	Dry powder	3330 mg of CuCl ₂ ·2H ₂ O was diluted with 333.3 mL isopropyl alcohol	10 mg/mL	Innovative Science
MgO	99.99	Dry powder	500 mg of MgO was diluted with 50mL isopropyl alcohol	10 mg/mL	Aqua Resources Corp
ZnO	99.99	Slurry dispersed in water: 20 wt.% ZnO and 80 wt.% water	2 mL of ZnO was diluted with 48 mL of isopropyl alcohol	10 mg/mL	American Elements
Cu(OH) ₂	99.99	Slurry dispersed in water: 22.25 wt.% Cu(OH) ₂ and 77.75 wt.% water	1.75 mL of Cu(OH) ₂ was diluted with 48.25 mL of isopropyl alcohol	10 mg/mL	Aqua Resources Corp

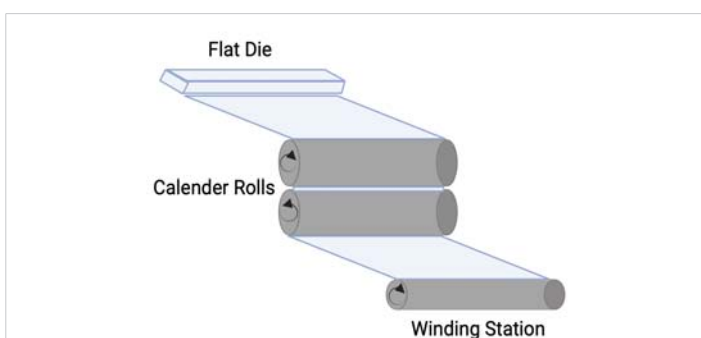


Figure 1: Cast film extrusion technique.



Figure 3: Schematic illustration demonstrating the use of Al foil is used before the compression molding process. Remodified with permission from ref. [32], Elsevier License No: 5754640428921. Copyright (2023) John Wiley and Sons.

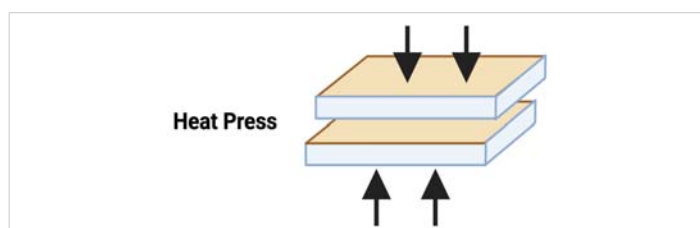


Figure 4: Schematic of the compression molding process.

Table 2: The metallic rod applicator's specification.

BAR No.	Color Code	Wire Diameter		Wet Film Deposit
		Inch	mm	Micron
0	White	0.002	0.05	4
1	Yellow	0.003	0.08	6
2	Red	0.006	0.15	12
3	Green	0.012	0.30	24
4	Black	0.020	0.51	40
5	Horn	0.025	0.64	50
6	Orange	0.030	0.76	60
7	Brown	0.040	1.02	80
8	Blue	0.050	1.27	100
9	Tan	0.060	1.52	120

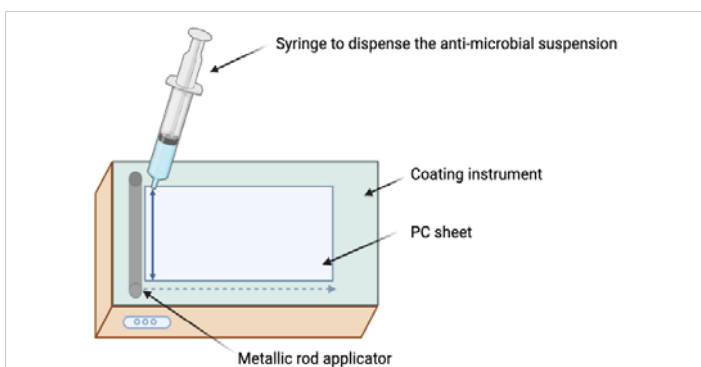


Figure 2: Deposition of the anti-microbial suspension onto a substrate using a metallic rod applicator.

Data analysis method

The statistical analysis was performed individually for each selected anti-microbial coating agent to understand whether there is an effect due to the change in coating concentration (ppm), coating thickness (µm), and the interaction between these two factors on the anti-microbial properties on the coated disks. In addition, a complete analysis was performed on all agents to rank the best agent in terms of the highest anti-microbial performance against *E. coli* K-12 MG1655 at two time intervals (4 and 24 hrs).

Statistical design

A 2x2x6 full-factorial experiment was used to investigate the effects of coating concentrations of (3000 and 10,000 ppm), MRA No. 3 and 5 that correspond to a wet film coating thickness of (24 and 50 µm), respectively, and six types of anti-microbial agents (Cu-infused Mg(OH)₂, Mg(OH)₂, Cu(OH)₂, MgO, CuCl₂·2H₂O, and ZnO) on the growth of *E. coli* K-12 MG1655 at two-time intervals (4 and 24 hrs). All experiments were independently replicated three times. Differences in the growth of *E. coli* K-12 MG1655 as affected by coating concentration (ppm), and coating thickness (µm) of the anti-

microbial agents were estimated using repeated measures (MANOVA) on JMP software (JMP Pro 16.1.0 (539038), SAS Institute Inc, Cary, North Carolina, USA).

Results and discussion

Thermally embossed PC disks with Cu-infused Mg(OH)₂ particles

The Cu-infused Mg(OH)₂ crystals have a green color. It is an anti-microbial agent consisting of a mixture of copper (Cu) and magnesium hydroxide (Mg(OH)₂) compounds which was developed by Aqua Recourses Crop, Fort Walton Beach, FL, USA, (Patent No: US20220225610A1) [33]. Each compound has a different particle shape and size, and they are attached together with the outer surface of each particle (this was checked and confirmed by SEM and EDX in our lab, data is not provided). The platelet-shaped particles represent the Mg(OH)₂ and were in the range of 160 nm - 260 nm by width and the range of 30 nm - 50 nm by thickness, while the spherical shape particles represent the Cu and were in the diameter range of 100 nm - 280 nm. The anti-microbial data obtained for neat PC disks, and PC disks coated with varying concentrations (ppm) and thicknesses (μm) of Cu-infused Mg(OH)₂ are presented in Figure 5 and Table 3.

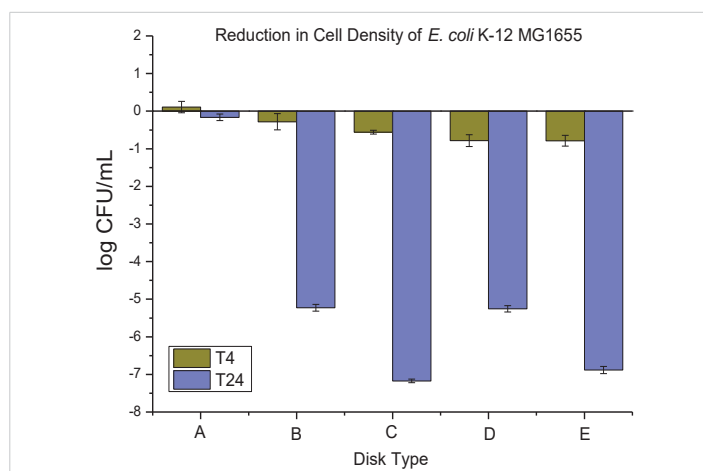


Figure 5: The anti-microbial data obtained for (A) neat PC disks, and PC disks coated with varying concentration (ppm) and thickness (μm) of Cu-infused Mg(OH)₂, (B) PC disks coated with (10,000 ppm and MRA No. 5 ~ 50 μm), (C) PC disks coated with (10,000 ppm and MRA No. 3 ~ 24 μm), (D) PC disks coated with (3000 ppm and MRA No. 5 ~ 50 μm), and PC disks coated with (3000 ppm and MRA No. 3 ~ 24 μm). Note: MRA refers to the metallic road applicator's number (MRA No. 3 and 5 which corresponds to a wet coating film of 24 and 50 μm, respectively).

Table 3: Changes in the population of *E. coli* K-12 MG1655 caused by the coated plastic disks with Cu-infused Mg(OH)₂ particles at 4 and 24 hrs.

Disk Type	<i>E. coli</i> Population (log CFU/mL) ± SEM	
	T-4 change	T-24 change
A Neat PC disks	0.11 ± 0.15	-0.16 ± 0.09
B PC disks coated with (10,000 ppm and MRA No. 5 ~ 50 μm)	-0.79 ± 0.14	-6.88 ± 0.10
C PC disks coated with (10,000 ppm and MRA No. 3 ~ 24 μm)	-0.78 ± 0.16	-5.26 ± 0.08
D PC disks coated with (3000 ppm and MRA No. 5 ~ 50 μm)	-0.56 ± 0.05	-7.17 ± 0.05
E PC disks coated with (3000 ppm and MRA No. 3 ~ 24 μm)	-0.28 ± 0.22	-5.23 ± 0.09

The neat PC disks were found to cause an increase of 0.11 ± 0.15 in 4 hrs, and a reduction of 0.16 ± 0.09 log CFU per mL of *E. coli* K-12 MG1655 in 24 hrs. The (10,000 ppm, and MRA No. 5 ~ 50 μm) coating concentration and coating thickness of Cu-infused Mg(OH)₂ were found to cause a 0.79 ± 0.14, and 6.88 ± 0.10 log CFU reduction per mL of *E. coli* K-12 MG1655 in 4 and 24 hrs respectively. The (10,000 ppm, and MRA No. 3 ~ 24 μm) coating concentration and coating thickness of Cu-infused Mg(OH)₂ were found to cause a 0.78 ± 0.16, and 5.26 ± 0.08 log CFU reduction per mL of *E. coli* K-12 MG1655 in 4 and 24 hrs, respectively. The (3000 ppm, and MRA No. 5 ~ 50 μm) coating concentration and coating thickness of Cu-infused Mg(OH)₂ were found to cause a 0.56 ± 0.05, and 7.17 ± 0.05 log CFU reduction per mL of *E. coli* K-12 MG1655 in 4 and 24 hrs, respectively. The (3000 ppm, and MRA No. 3 ~ 24 μm) coating concentration and coating thickness of Cu-infused Mg(OH)₂ were found to cause a 0.28 ± 0.22, and 5.23 ± 0.09 log CFU reduction per mL of *E. coli* K-12 MG1655 in 4 and 24 hrs respectively.

Thermally embossed PC disks with Mg(OH)₂ particles

The Mg(OH)₂ crystals have a white color. The particles were platelets in shape, and they were approximately 160 nm - 260 nm wide with a 30 nm - 50 nm thickness (this was checked and confirmed by SEM and EDX in our lab, data is not provided) which was developed by Aqua Recourses Crop, Fort Walton Beach, FL, USA, (Patent No: US20080171158A1) [34]. The anti-microbial data obtained for neat PC disks, and PC disks coated with varying concentrations (ppm) and thickness (μm) of Mg(OH)₂ are presented in Figure 6 and Table 4.

The neat PC disks were found to cause an increase of 0.40 ± 0.15 in 4 hrs, and a reduction of -0.13 ± 0.09 log CFU per mL of *E. coli* K-12 MG1655 in 24 hrs. The (10,000 ppm, and MRA No. 5 ~ 50 μm) coating concentration and coating thickness of Mg(OH)₂ were found to cause a 1.55 ± 0.26, and 5.45 ± 0.12 log CFU reduction per mL of *E. coli* K-12 MG1655 in 4 and

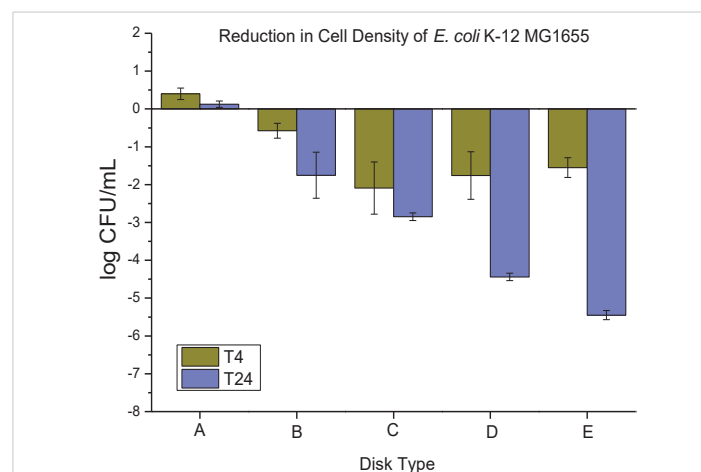


Figure 6: The anti-microbial data obtained for (A) neat PC disks, and PC disks coated with varying concentration (ppm) and thickness (μm) of Mg(OH)₂, (B) PC disks coated with (10,000 ppm and MRA No. 5 ~ 50 μm), (C) PC disks coated with (10,000 ppm and MRA No. 3 ~ 24 μm), (D) PC disks coated with (3000 ppm and MRA No. 5 ~ 50 μm), and PC disks coated with (3000 ppm and MRA No. 3 ~ 24 μm).

Table 4: Changes in the population of *E. coli* K-12 MG1655 were caused by the coated plastic disks with Mg(OH)₂ particles at 4 and 24 hrs.

	Disk Type	<i>E. coli</i> Population (log CFU/mL) ± SEM	
		T-4 change	T-24 change
A	Neat PC disks	0.40 ± 0.15	-0.13 ± 0.09
B	PC disks coated with (10,000 ppm and MRA No. 5 ~ 50 μ)	-1.55 ± 0.26	-5.45 ± 0.12
C	PC disks coated with (10,000 ppm and MRA No. 3 ~ 24 μ)	-1.76 ± 0.63	-4.44 ± 0.10
D	PC disks coated with (3000 ppm and MRA No. 5 ~ 50 μ)	-2.09 ± 0.69	-2.85 ± 0.10
E	PC disks coated with (3000 ppm and MRA No. 3 ~ 24 μ)	-0.58 ± 0.20	-1.75 ± 0.61

24 hrs, respectively. The (10,000 ppm, and MRA No. 3 ~ 24 μ) coating concentration and coating thickness of Mg(OH)₂ were found to cause a 1.76 ± 0.63, and 4.44 ± 0.10 log CFU reduction per mL of *E. coli* K-12 MG1655 in 4 and 24 hrs, respectively. The (3000 ppm, and MRA No. 5 ~ 50 μ) coating concentration and coating thickness of Mg(OH)₂ were found to cause a 2.09 ± 0.69, and 2.85 ± 0.10 log CFU reduction per mL of *E. coli* K-12 MG1655 in 4 and 24 hrs, respectively. The (3000 ppm, and MRA No. 3 ~ 24 μ) coating concentration and coating thickness of Mg(OH)₂ were found to cause a 0.58 ± 0.20, and 1.75 ± 0.61 log CFU reduction per mL of *E. coli* K-12 MG1655 in 4 and 24 hrs, respectively.

Thermally embossed PC disks with CuCl₂·2H₂O particles

The CuCl₂·2H₂O crystals have a green color. The particles were lath-like in shape, and were in the range of 34-336 μm in length with a thickness of approximately 19-50 μm (this was checked and confirmed by SEM and EDX in our lab, data is not provided). The anti-microbial data obtained for neat PC disks, and PC disks coated with varying concentrations (ppm) and thickness (μm) of CuCl₂·2H₂O are presented in Figure 7 and Table 5.

The neat PC disks were found to cause a 0.11 ± 0.15, and 0.38 ± 0.09 log CFU reduction per mL of *E. coli* K-12 MG1655 in 4 and 24 hrs, respectively. The (10,000 ppm, and MRA No. 5 ~ 50 μ) coating concentration and coating thickness of CuCl₂·2H₂O were found to cause a 0.90 ± 1.13, and 6.27 ± 0.07 log CFU reduction per mL of *E. coli* K-12 MG1655 in 4 and 24 hrs, respectively. The (10,000 ppm, and MRA No. 3 ~ 24 μ) coating concentration and coating thickness of CuCl₂·2H₂O were found to cause a 0.76 ± 0.07, and 2.37 ± 0.29 log CFU reduction per mL of *E. coli* K-12 MG1655 in 4 and 24 hrs, respectively. The (3000 ppm, and MRA No. 5 ~ 50 μ) coating concentration and coating thickness of CuCl₂·2H₂O were found to cause a 0.36 ± 0.61, and 3.08 ± 0.39 log CFU reduction per mL of *E. coli* K-12 MG1655 in 4 and 24 hrs, respectively. The (3000 ppm, and MRA No. 3 ~ 24 μ) coating concentration and coating thickness of CuCl₂·2H₂O were found to cause a 0.47 ± 0.54, and 1.87 ± 0.41 log CFU reduction per mL of *E. coli* K-12 MG1655 in 4 and 24 hrs, respectively.

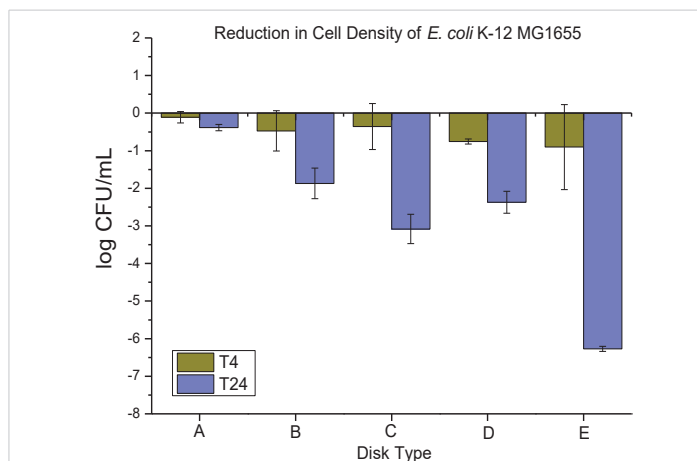


Figure 7: The anti-microbial data obtained for (A) neat PC disks, and PC disks coated with varying concentrations (ppm) and thickness (μm) of CuCl₂·2H₂O, (B) PC disks coated with (10,000 ppm and MRA No. 5 ~ 50 μ), (C) PC disks coated with (10,000 ppm and MRA No. 3 ~ 24 μ), (D) PC disks coated with (3000 ppm and MRA No. 5 ~ 50 μ), and PC disks coated with (3000 ppm and MRA No. 3 ~ 24 μ).

Table 5: Changes in the population of *E. coli* K-12 MG1655 were caused by the coated plastic disks with CuCl₂·2H₂O particles at 4 and 24 hrs.

	Disk Type	<i>E. coli</i> Population (log CFU/mL) ± SEM	
		T-4 change	T-24 change
A	Neat PC disks	-0.11 ± 0.15	-0.38 ± 0.09
B	PC disks coated with (10,000 ppm and MRA No. 5 ~ 50 μ)	-0.90 ± 1.13	-6.27 ± 0.07
C	PC disks coated with (10,000 ppm and MRA No. 3 ~ 24 μ)	-0.76 ± 0.07	-2.37 ± 0.29
D	PC disks coated with (3000 ppm and MRA No. 5 ~ 50 μ)	-0.36 ± 0.61	-3.08 ± 0.39
E	PC disks coated with (3000 ppm and MRA No. 3 ~ 24 μ)	-0.47 ± 0.54	-1.87 ± 0.41

Thermally embossed PC disks with MgO particles

Magnesium oxide (MgO) is the oxide salt of magnesium. It has white-colored micro-sized particles. MgO nanoparticles formed spherical agglomerates comprised of angular flakes. Flake size ranged between 50 nm - 200 nm; spherical agglomerates of MgO flakes measured 1-6 μm in diameter (this was checked and confirmed by SEM and EDX in our lab, data is not provided). The anti-microbial data obtained for neat PC disks, and PC disks coated with varying concentrations (ppm) and thickness (μm) of MgO are presented in Figure 8 and Table 6.

The neat PC disks were found to cause a 0.32 ± 0.15, and 0.59 ± 0.09 log CFU reduction per mL of *E. coli* K-12 MG1655 in 4 and 24 hrs, respectively. The (10,000 ppm, and MRA No. 5 ~ 50 μ) coating concentration and coating thickness of MgO was found to cause a 0.0033 ± 1.22, and 1.96 ± 0.05 log CFU reduction per mL of *E. coli* K-12 MG1655 in 4 and 24 hrs, respectively. The (10,000 ppm, and MRA No. 3 ~ 24 μ) coating concentration and coating thickness of MgO was found to cause a 1.02 ± 0.24, and 2.15 ± 0.59 log CFU reduction per mL of *E. coli* K-12 MG1655 in 4 and 24 hrs, respectively. The (3000 ppm, and MRA No. 5 ~ 50 μ) coating concentration and coating thickness of MgO was found to cause a 1.22 ±

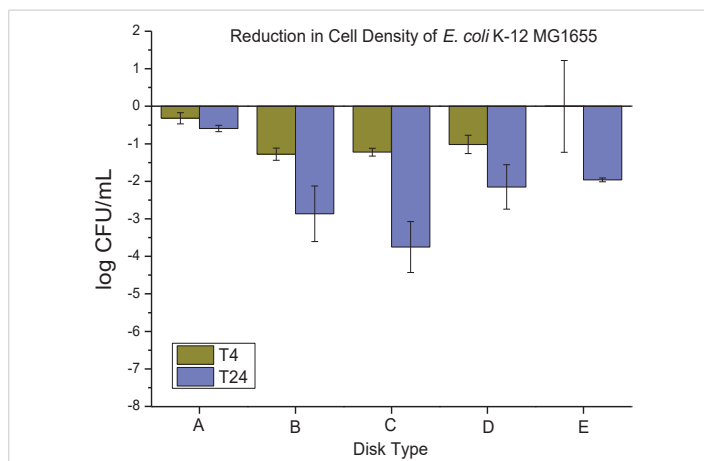


Figure 8: The anti-microbial data obtained for (A) neat PC disks, and PC disks coated with varying concentration (ppm) and thickness (μm) of MgO, (B) PC disks coated with (10,000 ppm and MRA No. 5 ~ 50 μm), (C) PC disks coated with (10,000 ppm and MRA No. 3 ~ 24 μm), (D) PC disks coated with (3000 ppm and MRA No. 5 ~ 50 μm), and PC disks coated with (3000 ppm and MRA No. 3 ~ 24 μm).

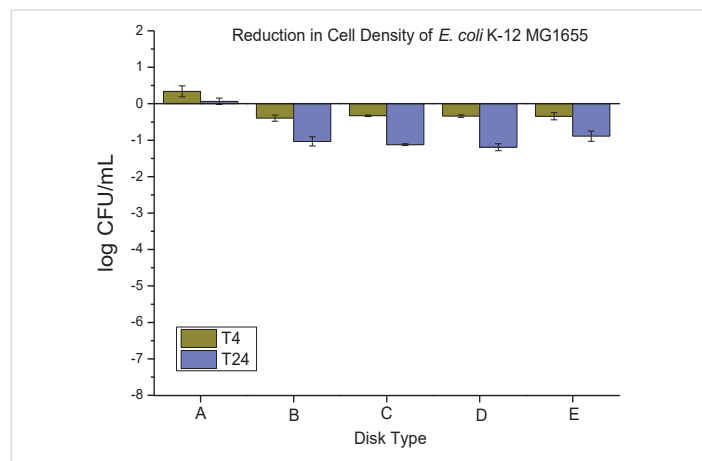


Figure 9: The anti-microbial data obtained for (A) neat PC disks, and PC disks coated with varying concentrations (ppm) and thickness (μm) of ZnO, (B) PC disks coated with (10,000 ppm and MRA No. 5 ~ 50 μm), (C) PC disks coated with (10,000 ppm and MRA No. 3 ~ 24 μm), (D) PC disks coated with (3000 ppm and MRA No. 5 ~ 50 μm), and PC disks coated with (3000 ppm and MRA No. 3 ~ 24 μm).

Table 6: Changes in the population of *E. coli* K-12 MG1655 were caused by the coated plastic disks with MgO particles at 4 and 24 hrs.

Disk Type	<i>E. coli</i> Population (log CFU/mL) ± SEM	
	T-4 change	T-24 change
A Neat PC disks	-0.32 ± 0.15	-0.59 ± 0.09
B PC disks coated with (10,000 ppm and MRA No. 5 ~ 50 μm)	-0.0033 ± 1.22	-1.96 ± 0.05
C PC disks coated with (10,000 ppm and MRA No. 3 ~ 24 μm)	-1.02 ± 0.24	-2.15 ± 0.59
D PC disks coated with (3000 ppm and MRA No. 5 ~ 50 μm)	-1.22 ± 0.10	-3.75 ± 0.68
E PC disks coated with (3000 ppm and MRA No. 3 ~ 24 μm)	-1.28 ± 0.16	-2.87 ± 0.74

Table 7: Changes in the population of *E. coli* K-12 MG1655 were caused by the coated plastic disks with ZnO particles at 4 and 24 hrs.

Disk Type	<i>E. coli</i> Population (log CFU/mL) ± SEM	
	T-4 change	T-24 change
A Neat PC disks	0.34 ± 0.15	0.67 ± 0.09
B PC disks coated with (10,000 ppm and MRA No. 5 ~ 50 μm)	-0.34 ± 0.10	-0.89 ± 0.14
C PC disks coated with (10,000 ppm and MRA No. 3 ~ 24 μm)	-0.34 ± 0.04	-1.19 ± 0.10
D PC disks coated with (3000 ppm and MRA No. 5 ~ 50 μm)	-0.33 ± 0.02	-1.12 ± 0.03
E PC disks coated with (3000 ppm and MRA No. 3 ~ 24 μm)	-0.40 ± 0.09	-1.03 ± 0.13

0.10, and 3.75 ± 0.68 log CFU reduction per mL of *E. coli* K-12 MG1655 in 4 and 24 hrs, respectively. The (3000 ppm, and MRA No. 3 ~ 24 μm) coating concentration and coating thickness of MgO was found to cause a 1.28 ± 0.16 , and 2.87 ± 0.74 log CFU reduction per mL of *E. coli* K-12 MG1655 in 4 and 24 hrs, respectively.

Thermally embossed PC disks with ZnO particles

Zinc Oxide (ZnO), nanodispersion, APS 30 nm - 40 nm, Concentration: 20 wt.% ZnO in water. ZnO nanoparticles had a rounded shape measuring approximately 10 nm - 25 nm (this was checked and confirmed by SEM and EDX in our lab, data is not provided). The anti-microbial data obtained for neat PC disks, and PC disks coated with varying concentrations (ppm) and thickness (μm) of ZnO are presented in Figure 9 and Table 7.

The neat PC disks were found to cause an increase of 0.34 ± 0.15 , and 0.67 ± 0.09 log CFU per mL of *E. coli* K-12 MG1655 in 4 and 24 hrs, respectively. The (10,000 ppm, and MRA No. 5 ~ 50 μm) coating concentration and coating thickness of ZnO was found to cause a 0.34 ± 0.10 , and 0.89 ± 0.14 log CFU reduction per mL of *E. coli* K-12 MG1655 in 4 and 24 hrs, respectively. The (10,000 ppm, and MRA No. 3 ~ 24 μm) coating concentration and coating thickness of ZnO was found

to cause a 0.34 ± 0.04 , and 1.19 ± 0.10 log CFU reduction per mL of *E. coli* K-12 MG1655 in 4 and 24 hrs, respectively. The (3000 ppm, and MRA No. 5 ~ 50 μm) coating concentration and coating thickness of ZnO was found to cause a 0.33 ± 0.02 , and 1.12 ± 0.03 log CFU reduction per mL of *E. coli* K-12 MG1655 in 4 and 24 hrs, respectively. The (3000 ppm, and MRA No. 3 ~ 24 μm) coating concentration and coating thickness of ZnO was found to cause a 0.40 ± 0.09 , and 1.03 ± 0.13 log CFU reduction per mL of *E. coli* K-12 MG1655 in 4 and 24 hrs, respectively.

Thermally embossed PC disks with Cu(OH)₂ particles

Copper (II) hydroxide is the hydroxide of copper with the chemical formula of Cu(OH)₂. It has a pale greenish-blue color. Cu(OH)₂ appeared in two distinct sizes; large rectangular crystals greater than 500 nm in length were mixed with small rectangular nanoparticles 20 nm - 50 nm in size (this was checked and confirmed by SEM and EDX in our lab, data is not provided). The anti-microbial data obtained for neat PC disks, and PC disks coated with varying concentrations (ppm) and thickness (μm) of Cu(OH)₂ are presented in Figure 10 and Table 8.

The neat PC disks were found to cause a 0.11 ± 0.15 , and 0.38 ± 0.09 log CFU reduction per mL of *E. coli* K-12 MG1655

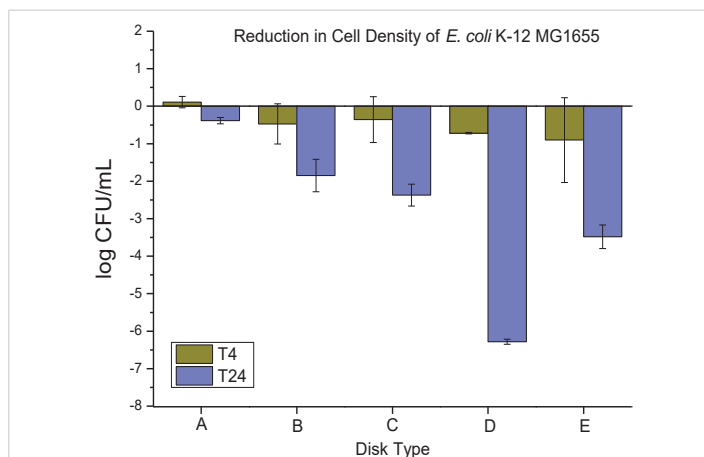


Figure 10: The anti-microbial data obtained for (A) neat PC disks, and PC disks coated with varying concentrations (ppm) and thickness (μm) of Cu(OH)₂, (B) PC disks coated with (10,000 ppm and MRA No. 5 ~ 50 μm), (C) PC disks coated with (10,000 ppm and MRA No. 3 ~ 24 μm), (D) PC disks coated with (3000 ppm and MRA No. 5 ~ 50 μm), and PC disks coated with (3000 ppm and MRA No. 3 ~ 24 μm).

Table 8: Changes in the population of *E. coli* K-12 MG1655 were caused by the coated plastic disks with Cu(OH)₂ particles at 4 and 24 hrs.

Disk Type	<i>E. coli</i> Population (log CFU/mL) ± SEM	
	T-4 change	T-24 change
A Neat PC disks	-0.11 ± 0.15	-0.38 ± 0.09
B PC disks coated with (10,000 ppm and MRA No. 5 ~ 50 μm)	-0.90 ± 1.13	-3.48 ± 0.32
C PC disks coated with (10,000 ppm and MRA No. 3 ~ 24 μm)	-0.72 ± 0.02	-6.28 ± 0.07
D PC disks coated with (3000 ppm and MRA No. 5 ~ 50 μm)	-0.36 ± 0.61	-2.37 ± 0.29
E PC disks coated with (3000 ppm and MRA No. 3 ~ 24 μm)	-0.47 ± 0.54	-1.85 ± 0.43

in 4 and 24 hrs respectively. The (10,000 ppm, and MRA No. 5 ~ 50 μm) coating concentration and coating thickness of Cu(OH)₂ were found to cause a 0.90 ± 1.13, and 3.48 ± 0.32 log CFU reduction per mL of *E. coli* K-12 MG1655 in 4 and 24 hrs, respectively. The (10,000 ppm, and MRA No. 3 ~ 24 μm) coating concentration and coating thickness of Cu(OH)₂ were found to cause a 0.72 ± 0.02, and 6.28 ± 0.07 log CFU reduction per mL of *E. coli* K-12 MG1655 in 4 and 24 hrs, respectively. The (3000 ppm, and MRA No. 5 ~ 50 μm) coating concentration and coating thickness of Cu(OH)₂ were found to cause a 0.36 ± 0.61, and 2.37 ± 0.29 log CFU reduction per mL of *E. coli* K-12 MG1655 in 4 and 24 hrs, respectively. The (3000 ppm, and MRA No. 3 ~ 24 μm) coating concentration and coating thickness of Cu(OH)₂ were found to cause a 0.47 ± 0.54, and 1.85 ± 0.43 log CFU reduction per mL of *E. coli* K-12 MG1655 in 4 and 24 hrs, respectively.

Overall summary

The coating concentration (ppm) was found to be a significant factor affecting the anti-microbial performance for Cu-infused Mg(OH)₂, Mg(OH)₂, Cu(OH)₂, MgO, CuCl₂·2H₂O, and ZnO ($p = 0.004, p < 0.0001, p < 0.0001, p = 0.0297, p = 0.0011,$ and $p = 0.0130$ respectively).

The coating thickness (μm) was found to be a major

significant contributor to the anti-microbial properties of Cu-infused Mg(OH)₂, Mg(OH)₂, Cu(OH)₂, MgO, and CuCl₂·2H₂O ($p < 0.0001, p = 0.0004, p = 0.0011, p = 0.0310,$ and $p < 0.0001$ respectively). It was not a significant factor for ZnO.

The interaction between the coating concentration (ppm), and the coating thickness (μm) was found to be a significant factor for Cu-infused Mg(OH)₂, Cu(OH)₂, MgO, CuCl₂·2H₂O, and ZnO ($p < 0.0001, p = 0.0001, p = 0.0004, p < 0.0001,$ and $p < 0.0001$ respectively). It was not a significant factor for Mg(OH)₂.

Anti-microbial agent's ranking

The ranking of agents was based on the statistical analysis of the GroupWise coefficient of each agent from the parameter estimates for the average coating concentration (6500 ppm) and the average MRA No. 4 ~ 40 μm in a repeated measure (MANOVA) at time T=24. Each coefficient was significantly different from the neat plastic treatment ($p < 0.001$). The agent's largest to smallest reductions of *E. coli* K-12 MG1655 population were Cu-infused Mg(OH)₂, Cu(OH)₂, CuCl₂·2H₂O, Mg(OH)₂, MgO, and ZnO as presented in Figure 11.

The analysis was conducted using repeated measures (MANOVA) to make group comparisons. The model for the (MANOVA) analysis was as follows:

$$Y_{ijkl} = \alpha_i + \beta_{ij} + \bar{a}_{ik} + \beta\gamma_{ijk} + \tau_l + \epsilon_{ijkl}$$

Where α_i is the coefficient of the treatment i, β_{ij} is the random effect of treatment concentration for treatment i, γ_{ik} is the random effect of treatment thickness for treatment $i, \beta\gamma_{ijk}$ is the interaction of coating concentration and thickness for treatment i, τ_l the effect of time l and ϵ_{ijkl} is an experimental error.

Model estimate

Model parameter estimates were calculated for each of the six treatments individually using repeated measure (MANOVA) for each treatment as presented in Table 9. The six models for the (MANOVA) analysis were as follows:

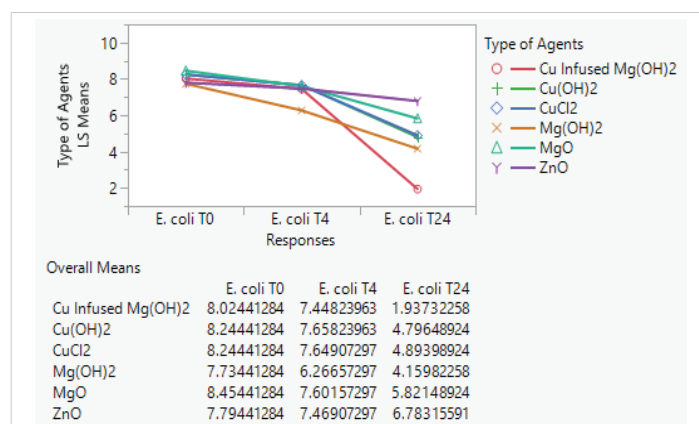


Figure 11: The least-square means for six types of agents over three time periods (T0, T4, and T24).



Table 9: The addition effect values of coating concentration (PPM), MAR No. coating thickness (µm), and the interaction between these two factors on the anti-microbial properties at 4 and 24 hrs for the six selected agents.

Agents	Disk Type		Coating Thickness (µ)		Interaction	
	4 h	24 h	4 h	24 h	4 h	24 h
Cu-infused Mg(OH) ₂	-5.600x 10 ⁻⁵	-5.348 x 10 ⁻⁵	-6.043 x 10 ⁻²	-1.086	8.552 x 10 ⁻⁶	7.424 x 10 ⁻⁵
Mg(OH) ₂	-6.279 x 10 ⁻⁵	-3.554 x 10 ⁻⁴	2.395 x 10 ⁻¹	-4.522 x 10 ⁻¹	N.S.	N.S.
Cu(OH) ₂	-5.703 x 10 ⁻⁵	-4.922 x 10 ⁻⁴	-4.190 x 10 ⁻²	5.459 x 10 ⁻¹	4.758 x 10 ⁻⁶	1.479 x 10 ⁻⁴
MgO	1.511 x 10 ⁻⁵	1.019 x 10 ⁻⁴	-4.448 x 10 ⁻³	3.210 x 10 ⁻¹	4.761 x 10 ⁻⁵	9.174 x 10 ⁻⁵
CuCl ₂ .2H ₂ O	-6.064 x 10 ⁻⁵	1.429 x 10 ⁻⁴	-3.280 x 10 ⁻²	-1.130	-3.186 x 10 ⁻⁶	-1.606 x 10 ⁻⁴
ZnO	-1.826 x 10 ⁻⁵	-3.525 x 10 ⁻⁵	-5.456 x 10 ⁻²	-3.782 x 10 ⁻²	1.915 x 10 ⁻⁵	4.525 x 10 ⁻⁵

$$Y_{ijkl} = \alpha_i + \beta_{ij} + \gamma_{ik} + \beta\gamma_{ijk} + \epsilon_{ijkl}$$

Where β_j is the random effect of treatment concentration for the treatment, γ_k is the random effect of treatment thickness for the treatment, $\beta\gamma_{jk}$ is the interaction of coating concentration and thickness for the treatment, τ_l effect of time l , and ϵ_{jkl} is an experimental error.

The addition of 1 ppm on the coating concentration of (Cu-infused Mg(OH)₂, Mg(OH)₂, Cu(OH)₂, MgO, CuCl₂.2H₂O, and ZnO) will cause (-5.600x10⁻⁵, -6.279x10⁻⁵, -5.703x10⁻⁵, 1.511x10⁻⁵, -6.064x10⁻⁵, and -1.826x10⁻⁵, respectively) on the *E.coli* cell density in 4 hrs, and (-5.348x10⁻⁵, -3.554x10⁻⁴, -4.922x10⁻⁴, 1.019x10⁻⁴, -1.429x10⁻⁴, and -3.525x10⁻⁵, respectively) in 24 hrs.

The effect of a MRA No. 1 increase (Table 1) on the coating thickness of (Cu-infused Mg(OH)₂, Mg(OH)₂, Cu(OH)₂, MgO, CuCl₂.2H₂O, and ZnO) will cause (-6.043x10⁻², -2.395x10⁻¹, -4.190x10⁻², -4.448x10⁻³, -3.280x10⁻², and -5.456x10⁻², respectively) on the *E.coli* cell density in 4 hrs, and (-1.086, -4.522x10⁻¹, 5.459x10⁻¹, -3.210x10⁻¹, -1.130, and -3.782x10⁻², respectively) in 24 hrs.

The interaction between coating concentration and coating thickness is significant for all agents except Mg(OH)₂.

Conclusion

The coating concentration (ppm) was a significant substantial factor for all agents. The coating thickness (µm) was a significant factor for all agents except ZnO. The interaction between the coating concentration (ppm), and the coating thickness (µm) was significant for all agents except Mg(OH)₂.

The most effective agent at 4 hrs was Mg(OH)₂; the other agents were all similar. At 24 hrs, Mg(OH)₂ became the second most effective agent and Cu-infused Mg(OH)₂ was the most effective agent. The other agents in order from most to least effective were CuCl₂.2H₂O, Mg(OH)₂, MgO, and ZnO.

Each agent increased effectiveness as the coating concentration and the coating thickness increased. The parameter estimates for each coating agent allowed the estimation of *E.coli* decrease for any desired coating concentration and coating thickness.

Acknowledgment

Saleh Alkarri would like to express his gratitude to the SABIC company, who generously funded his doctoral studies and all of his research needs at Michigan State University. He also thank Tariq Syed from SABIC T&I, John Cairney from Aqua Recourses Corp, and Gregory Neff from Purdue University for their contribution to proofreading these materials.

Conflicts of interest

The author declare that the research was conducted in the absence of any commercial or financial relationships that could be construed as a potential conflict of interest.

References

- Tuson HH, Weibel DB. Bacteria-surface interactions. *Soft Matter*. 2013 Sep 28;9(18):4368-4380. DOI: 10.1039/c3sm27705d.
- Kimkes TEP, Heinemann M. How bacteria recognise and respond to surface contact. *FEMS Microbiol Rev*. 2020 Jan 1;44(1):106-122. doi: 10.1093/femsre/fuz029. PMID: 31769807; PMCID: PMC7053574.
- Sacher E. Comment on "High-Resolution Microscopical Studies of Contact Killing Mechanisms on Copper-Based Surfaces". *ACS Appl Mater Interfaces*. 2022 Apr 20; 14(15):16959-16960.
- Stephens B, Azimi P, Thoemmes MS, Heidarinejad M, Allen JG, Gilbert JA. Microbial Exchange via Fomites and Implications for Human Health. *Curr Pollut Rep*. 2019;5(4):198-213. doi: 10.1007/s40726-019-00123-6. Epub 2019 Aug 31. PMID: 34171005; PMCID: PMC7149182.
- Jose A, Gizdavic-Nikolaidis M, Swift S. Antimicrobial Coatings: Reviewing Options for Healthcare Applications. 2023 Jan; 3(1):145-174.
- LakshmiPriya T. Introduction to nanoparticles and analytical devices. 2021; 1-29.
- Mahanta U, Khandelwal M, Deshpande AS. Antimicrobial surfaces: a review of synthetic approaches, applicability and outlook. *J Mater Sci*. 2021;56(32):17915-17941. doi: 10.1007/s10853-021-06404-0. Epub 2021 Aug 10. PMID: 34393268; PMCID: PMC8354584.
- Pinho AC, Piedade AP. Polymeric Coatings with Antimicrobial Activity: A Short Review. *Polymers (Basel)*. 2020 Oct 24;12(11):2469. doi: 10.3390/polym12112469. PMID: 33114426; PMCID: PMC7692441.
- Qiu H, Si Z, Luo Y, Feng P, Wu X, Hou W, Zhu Y, Chan-Park MB, Xu L, Huang D. The Mechanisms and the Applications of Antibacterial Polymers in Surface Modification on Medical Devices. *Front Bioeng Biotechnol*. 2020 Nov 11;8:910. doi: 10.3389/fbioe.2020.00910. PMID: 33262975; PMCID: PMC7686044.
- Alves MM, Batista C, Mil-Homens D, Grenho L, Fernandes MH, Santos CF. Enhanced antibacterial activity of Rosehip extract-functionalized Mg(OH)₂ nanoparticles: An in vitro and in vivo study. *Colloids Surf B Biointerfaces*. 2022 Sep;217:112643. doi: 10.1016/j.colsurfb.2022.112643. Epub 2022 Jun 15. PMID: 35759895.
- Mieszkowska M, Grden M. Electrochemical deposition of nickel targets



- from aqueous electrolytes for medical radioisotope production in accelerators: a review. *J Solid State Electrochem.* 2021; 25. DOI: 10.1007/s10008-021-04950-w.
12. Auclair J, Turcotte P, Gagnon C, Peyrot C, Wilkinson KJ, Gagné F. The Influence of Surface Coatings of Silver Nanoparticles on the Bioavailability and Toxicity to *Elliptio complanata* Mussels. *J Nanomater.* 2019; 2019:7843025. doi: 10.1155/2019/7843025.
 13. Birkett M, Dover L, Cherian Lukose C, Wasy Zia A, Tambuwala MM, Serrano-Aroca Á. Recent Advances in Metal-Based Antimicrobial Coatings for High-Touch Surfaces. *Int J Mol Sci.* 2022 Jan 21;23(3):1162. doi: 10.3390/ijms23031162. PMID: 35163084; PMCID: PMC8835042.
 14. Zhou Q, Li G, Zhou Z, Qu Y, Chen R, Gao X, Xu W, Nie S, Tian C, Li R. Effect of Ni²⁺ concentration on microstructure and bonding capacity of electrodeless copper plating on carbon fibers. *J Alloys Compd.* 2021;863:158467.
 15. Bruenke J, Roschke I, Agarwal S, Riemann T, Greiner A. Quantitative Comparison of the Antimicrobial Efficiency of Leaching versus Nonleaching Polymer Materials. *Macromol Biosci.* 2016 May;16(5):647-54. doi: 10.1002/mabi.201500266. Epub 2016 Jan 25. PMID: 26806336.
 16. Alkarri S, Bin Saad H, Soliman M. On Antimicrobial Polymers: Development, Mechanism of Action, International Testing Procedures, and Applications. *Polymers (Basel).* 2024 Mar 11;16(6):771. doi: 10.3390/polym16060771. PMID: 38543377; PMCID: PMC10975620.
 17. Cyphert EL, von Recum HA. Emerging technologies for long-term antimicrobial device coatings: advantages and limitations. *Exp Biol Med (Maywood).* 2017 Apr;242(8):788-798. doi: 10.1177/1535370216688572. Epub 2017 Jan 1. PMID: 28110543; PMCID: PMC5407537.
 18. Mullen DC, Wan X, Takala TM, Saris PE, Moreira VM. Precision Design of Antimicrobial Surfaces. *Front Med Technol.* 2021 Feb 16;3:640929. doi: 10.3389/fmedt.2021.640929. PMID: 35047910; PMCID: PMC8757849.
 19. Cuadros-Rodríguez L, Lazúen-Muros M, Ruiz-Samblás C, Navas-Iglesias N. Leachables from plastic materials in contact with drugs. State of the art and review of current analytical approaches. *Int J Pharm.* 2020 Jun 15;583:119332. doi: 10.1016/j.ijpharm.2020.119332. Epub 2020 Apr 28. PMID: 32360549.
 20. Gonzalez-Martin C. Airborne Infectious Microorganisms. In: *Encyclopedia of Microbiology.* 2019:52-60.
 21. Goodoory VC, Black CJ, Ford AC. Efficacy of Senna and Magnesium Oxide for the Treatment of Chronic Idiopathic Constipation. *Am J Gastroenterol.* 2021 Jun 1;116(6):1352-1353. doi: 10.14309/ajg.0000000000001041. PMID: 33136565.
 22. Mokabber T, Cao HT, Norouzi N, van Rijn P, Pei YT. Antimicrobial Electrodeposited Silver-Containing Calcium Phosphate Coatings. *ACS Appl Mater Interfaces.* 2020 Feb 5;12(5):5531-5541. doi: 10.1021/acsami.9b20158. Epub 2020 Jan 14. PMID: 31894959; PMCID: PMC7252902.
 23. Darvish M, Ajji A. Effect of Polyethylene Film Thickness on the Antimicrobial Activity of Embedded Zinc Oxide Nanoparticles. *ACS Omega.* 2021 Sep 29;6(40):26201-26209. doi: 10.1021/acsomega.1c03223. PMID: 34660979; PMCID: PMC8515594.
 24. Kania H, Sipa J. Microstructure Characterization and Corrosion Resistance of Zinc Coating Obtained on High-Strength Grade 10.9 Bolts Using a New Thermal Diffusion Process. *Materials (Basel).* 2019 Apr 29;12(9):1400. doi: 10.3390/ma12091400. PMID: 31032815; PMCID: PMC6539789.
 25. Lin J, Nguyen NT, Zhang C, Ha A, Liu HH. Antimicrobial Properties of MgO Nanostructures on Magnesium Substrates. *ACS Omega.* 2020 Sep 18;5(38):24613-24627. doi: 10.1021/acsomega.0c03151. PMID: 33015479; PMCID: PMC7528336.
 26. Alkarri S. Developing Methods for Incorporating Antimicrobial Biocidal Nanoparticles in Thermoplastics. Michigan State University, 2023.
 27. Nakamura Y, Okita K, Kudo D, Phuong DND, Iwamoto Y, Yoshioka Y, Ariyoshi W, Yamasaki R. Magnesium Hydroxide Nanoparticles Kill Exponentially Growing and Persister *Escherichia coli* Cells by Causing Physical Damage. *Nanomaterials (Basel).* 2021 Jun 16;11(6):1584. doi: 10.3390/nano11061584. PMID: 34208716; PMCID: PMC8234494.
 28. Okamoto K, Kudo D, Phuong DND, Iwamoto Y, Watanabe K, Yoshioka Y, Ariyoshi W, Yamasaki R. Magnesium Hydroxide Nanoparticles Inhibit the Biofilm Formation of Cariogenic Microorganisms. *Nanomaterials (Basel).* 2023 Feb 25;13(5):864. doi: 10.3390/nano13050864. PMID: 36903742; PMCID: PMC10005196.
 29. Vandebriel RJ, De Jong WH. A review of mammalian toxicity of ZnO nanoparticles. *Nanotechnol Sci Appl.* 2012 Aug 15;5:61-71. doi: 10.2147/NSA.S23932. PMID: 24198497; PMCID: PMC3781722.
 30. Halbus AF, Horozov TS, Paunov VN. Controlling the Antimicrobial Action of Surface Modified Magnesium Hydroxide Nanoparticles. *Biomimetics (Basel).* 2019 Jun 25;4(2):41. doi: 10.3390/biomimetics4020041. PMID: 31242662; PMCID: PMC6631741.
 31. Nguyen NT, Grelling N, Wetteland CL, Rosario R, Liu H. Antimicrobial Activities and Mechanisms of Magnesium Oxide Nanoparticles (nmGO) against Pathogenic Bacteria, Yeasts, and Biofilms. *Sci Rep.* 2018 Nov 2;8(1):16260. doi: 10.1038/s41598-018-34567-5. PMID: 30389984; PMCID: PMC6214931.
 32. Alkarri S, Sharma D, Bergholz TM, Rabnawaz M. Fabrication methodologies for antimicrobial polypropylene surfaces with leachable and nonleachable antimicrobial agents. *J Appl Polym Sci.* 2023; e54757.
 33. Maddan OL. Hydroxides monolayer nanoplatelet and methods of preparing same. Google Patents: 2022.
 34. Maddan OL. Nanoplatelet copper hydroxides and methods of preparing same. Google Patents: 2008.